# Ultracold thermalization of $^{7}$Li and $^{87}$Rb

C. Marzok, B. Deh, Ph. W. Courteille, and C. Zimmermann
*Physikalisches Institut, Eberhard-Karls-Universität Tübingen, Auf der Morgenstelle 14, D-72076 Tübingen, Germany*
(Received 18 May 2007; published 8 November 2007)

We report on measurements of cross-species thermalization inside a magnetically trapped spin-polarized mixture of $^{87}$Rb and $^{7}$Li atoms with both atoms in their respective low-field-seeking magnetic substates $|F=2,m_F=2\rangle$. Measurement of the thermalization velocity in the ultracold regime below 10 $\mu$K allows for the derivation of the absolute value of the pure triplet *s*-wave scattering length governing the interaction. We find $|a_{7,87}|=(59\pm19)a_{\mathrm{B}}$. We propose to study both species in the condensed regime to derive the sign of $a_{7,87}$. In this context, we present numerical solutions to the coupled Gross-Pitaevskii equation based on the hypothesis of a positive sign. According to the simulations, phase separation of the Li and Rb $|2,2\rangle$ clouds occurs along with a mean-field stabilization allowing for larger atom numbers of condensed $^{7}$Li atoms before collapse sets in. Observation of this mean-field stabilization would directly fix the sign of $a_{7,87}$. We discuss our results in the light of this proposal.

DOI: 10.1103/PhysRevA.76.052704 PACS number(s): 34.50.−s, 03.75.Mn, 32.80.Pj

## I. INTRODUCTION

Sympathetic cooling with an independent heat bath is a convenient tool to cool atomic clouds that cannot be cooled directly. Its application to Fermi-Bose mixtures led to a breakthrough in reaching the quantum degenerate regime with fully spin polarized fermionic atom clouds. The antisymmetry of the fermionic wave functions prohibits direct evaporative cooling due to missing *s*-wave scattering. Adding a second bosonic species that can have collisions with the fermionic species circumvents this difficulty. A range of different Fermi-Bose mixtures was brought to the degenerate regime employing this technique: $^{6}$Li+$^{7}$Li [1], $^{6}$Li+$^{23}$Na [2], $^{40}$K+$^{87}$Rb [3], $^{6}$Li+$^{87}$Rb [4], $^{3}$He+$^{4}$He [5]. For bosonic target species it is also interesting to be cooled by an independent cooling agent. Two $^{87}$Rb condensates in different hyperfine states $F$ could be produced by evaporation of atoms in the $F=2$ state while atoms in $F=1$ were passively cooled through thermalizing collisions [6]. Another example is $^{85}$Rb, whose intraspecies scattering length $a_{85}$ has a zero crossing at collision energies $E_{coll}/k_B\sim375$ $\mu$K. This prohibits direct evaporation of $^{85}$Rb starting with higher temperatures. The problem was overcome by sympathetically cooling $^{85}$Rb in a bath of $^{87}$Rb [7]. Sympathetic cooling down to quantum degeneracy of the target species was also realized in $^{41}$K+$^{87}$Rb [8,9] and recently in $^{39}$K+$^{87}$Rb [10], where again $^{87}$Rb served as coolant. Furthermore, interspecies scattering properties were determined in a mixture of $^{87}$Rb and $^{133}$Cs, which was brought to low temperatures with the same technique [11]. Mixtures of different isotopes of Yb [12] as well as Yb+$^{87}$Rb mixtures [13] are currently under examination as well.

When working with $^{7}$Li, it is important to note that Bose-Einstein condensates of this species are intrinsically unstable in the $|F,m_F\rangle=|2,2\rangle$ hyperfine state because the $^{7}$Li triplet scattering length $a_7=-23.7a_{\mathrm{B}}$ is negative. This instability and the maximum condensate size were predicted theoretically [14] and later confirmed experimentally [15]. The strong effects that negative scattering lengths have on condensates were also shown in the controlled destabilization [16] and the spectacular "bosenova" experiments [17] in Bose-Einstein condensates of $^{85}$Rb, where the strength and sign of the scattering length was rapidly changed by means of a Feshbach resonance. Our interest in cooling $^{7}$Li with $^{87}$Rb originates in the mean-field interaction in the regime where both species are Bose condensed. Depending on the strength of this interaction, it can strongly alter the stability conditions for $^{7}$Li Bose-Einstein condensates, as we show in a theoretical section of this paper.

Here, we report on the experimental realization of sympathetic cooling of $^{7}$Li in a bath of $^{87}$Rb. From controlled thermalization experiments in a temperature range from 10 $\mu$K to 2 $\mu$K we extract the interspecies scattering cross section $\sigma_{7,87}=4\pi a_{7,87}^2$. This fixes the absolute value of the triplet scattering length to $|a_{7,87}|=(59\pm19)a_{\mathrm{B}}$. Upon cooling further down, we reach criticality with respect to Bose-Einstein condensation in $^{7}$Li before $^{87}$Rb starts to condense. The $^{7}$Li criticality manifests itself in additional sudden losses of the $^{7}$Li atom number; as for our trap conditions, the atom number of the overcritical $^{7}$Li largely exceeds the atom number of stable $^{7}$Li condensates.

We also present numerical solutions of the coupled Gross-Pitaevskii equations of two interacting condensates of $^{7}$Li and $^{87}$Rb in spherically symmetric traps. Stabilization of the Li condensate for large Rb atom numbers is observed for a positive sign of $a_{7,87}$. Experimentally, observation of this effect can be expected when intra- and interspecies inelastic loss coefficients are small and the overlap is good. A precondition for this is that the relative gravitational sag is smaller than the Thomas-Fermi radii of the condensates involved. Hence, by observing the collapse of Li and the impact of the mean-field energy of Rb on the collapse in a regime where both species are condensed, it is, in principle, possible to determine the sign of the mutual interaction [18].

We structure the paper as follows: In Sec. II we briefly describe the apparatus and the experimental procedure used for cooling. In Sec. III, experimental results for crossed species thermalization are presented and the absolute value of the scattering length determined. Section IV presents experimental evidence that we are able to reach the critical tem-

 

perature for Bose-Einstein condensation of $^7$Li. Finally, Sec. V describes the numerical calculations for coupled $^7$Li and $^{87}$Rb condensates.

## II. EXPERIMENTAL SETUP

Our experimental setup is identical to the one described in [4] where we studied thermalization between fermionic $^6$Li and $^{87}$Rb, except for the fact that we now use the bosonic isotope of Li. As atom sources we use commercial dispensers with (enriched) $^{87}$Rb and a Zeeman slower for the $^7$Li. Up to $3\times10^8$ Rb and $8\times10^7$ Li atoms are simultaneously trapped in two spatially overlapping magneto-optical traps (MOTs). We then compress the MOTs by increasing the trap coil currents and then apply a short (1 ms) stage of polarization gradient cooling. The Rb then has a temperature of $T_{87}\approx80$ $\mu$K. The Li, for which polarization gradient cooling does not work because of the unresolved hyperfine structure in the excited state, has an estimated temperature of several hundred $\mu$K. Before turning on the magnetic trap, the Rb is optically pumped into the stretched state $|2,2\rangle$, while Li is left unpolarized. We magnetically trap almost all Rb atoms and approximately $10^7$ Li atoms [19]. The mixture is then adiabatically transferred via several intermediate magnetic traps into a Ioffe-Pritchard-type trap characterized by the secular frequencies $\tilde{\omega}_{87}/2\pi=(50\times206\times200)^{1/3}$ Hz for the Rb $|2,2\rangle$ state (for Li $|2,2\rangle$ the frequencies are higher by a factor $\sqrt{87/7}$) and the magnetic field offset 3 G. As in the case of $^6$Li, purity of the Rb spin states has to be ensured by special measures. Directly after turning on the Ioffe-Pritchard trap, a cleaning microwave sweep coupling residual Rb $|1,-1\rangle$ atoms to the untrapped $|2,-2\rangle$ state is applied. The Rb cloud is then selectively cooled by forced microwave evaporation coupling the $|2,2\rangle$ state with the antitrapped $|1,1\rangle$ state at a certain distance from the trap center. An additional microwave knife has to be applied that constantly empties the trap from $|2,1\rangle$ Rb atoms by coupling them to the untrapped $|1,0\rangle$ state. The $|2,1\rangle$ atoms accumulate during the last stages of evaporation via dipolar relaxation [20] and lead to severe losses in Li atom numbers through inelastic collisions. The Li cloud, which is not actively cooled, adjusts its temperature to the Rb cloud via interspecies thermalization. We find that $^7$Li thermalizes much faster than its fermionic counterpart $^6$Li [4]. Atom numbers and temperatures are derived by standard optical absorption imaging. The trap is rapidly turned off and the clouds expand ballistically for a variable amount of time. Light pulses resonant with the $F=2\rightarrow F'=3$ transitions of the respective $D_2$ lines then map the density distribution onto charge-coupled device (CCD) cameras. In the case of Li, an additional counterpropagating repumping beam resonant with the $F=1\rightarrow F'=2$ transition is applied to keep the atoms in the cycling transition for the absorption imaging. The purity of the samples with respect to Zeeman substates is monitored by application of a magnetic field gradient during ballistic expansion of the clouds.

## III. CROSS-SPECIES THERMALIZATION

To measure the interspecies thermalization speed, we perform experiments at three different temperatures. Each experiment consists of two stages. First, the mixture is slowly (20 s) cooled to a common temperature $T_1$. Then, a stage of rapid cooling (50 ms) follows, which leaves the Rb at a temperature $T_2$, thus producing a temperature difference between the two atomic ensembles. The thermalization of the Li in the colder Rb bath is used for determining the scattering length using a straight forward collision model [21]. The temperature ranges in the three measurements are $T_1$ ($\mu$K) $\rightarrow T_2$ ($\mu$K): $10\rightarrow6$, $6\rightarrow4$, and $4.5\rightarrow2$. On a time scale of 300 ms, thermalization is completed (see Fig. 1), which is considerably faster than for $^6$Li, where thermalization times on the order of 3 s were observed under similar conditions [4].

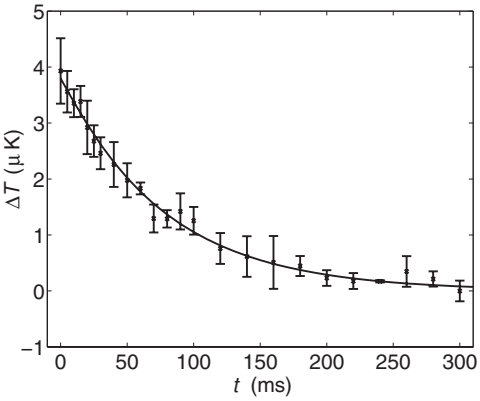


FIG. 1. Measured (data points) and simulated evolution (solid curve) of the thermalization process in the case of $T_1=10$ $\mu$K. After about 300 ms the thermalization process is complete. Each data point is an average of three individual measurements; the error bars indicate the statistical uncertainty.

It follows a short description of the thermalization model which we use to derive the scattering length. The total collision rate depends on the overlap integral of the two atomic clouds which, for purely thermal samples in harmonic traps, can be exactly solved [22] as

$$\Gamma_{coll}=\frac{\sigma_{7,87}}{(2\pi)^{3/2}}\bar{v}N_7N_{87}\left[\frac{m_7\tilde{\omega}_7^2}{k_B(T_7+T_{87})}\right]^{3/2}, \tag{1}$$

with the collision cross section $\sigma_{7,87}=4\pi a_{7,87}^2$, the interspecies pure triplet scattering length $a_{7,87}$, the mean trap frequency $\tilde{\omega}_7=(\omega_{7,r}^2\omega_{7,z})^{1/3}$, and the mean relative thermal velocity $\bar{v}=\sqrt{\frac{8k_B}{\pi}\left(\frac{T_7}{m_7}+\frac{T_{87}}{m_{87}}\right)}$. For atoms with equal masses, an average of 2.7 collisions is needed for thermalization [23]; however, in the case of unequal masses efficiency is reduced by a factor $\xi=\frac{4m_7m_{87}}{(m_7+m_{87})^2}$ [22]. In our case, Li needs $\sim10$ collisions to thermalize with the Rb. Here we assume the Rb temperature does not change during the thermalization process. We ensure this experimentally by application of a constant frequency microwave knife during the thermalization stage of the experiment which keeps the Rb temperature (but not the atom number) fixed. The temperature difference $\Delta T=T_7-T_{87}$ follows the differential equation

TABLE I. Resulting absolute scattering lengths for three different thermalization experiments. The quality of the fit $\chi^2$ is also shown. The variations in the derived scattering length show the limitation as to the accuracy in determining $|a_{7,87}|$ with this method. The mean value is $\bar{a}=59a_B$ with a standard deviation $\epsilon_{\bar{a}}=5.2a_B$. Further errors are discussed in the main text and Fig. 2.

| $T_1$ ($\mu$K) | $T_2$ ($\mu$K) | $\lvert a_{7,87}\rvert$ ($a_B$) | $\chi^2$ |
|---|---|---|---|
| 10 | 6 | 56 | 0.500 |
| 6 | 4 | 65 | 0.238 |
| 4.5 | 2 | 56 | 0.924 |

$$\frac{d(\Delta T)}{dt} = -\gamma \Delta T = -\frac{\Gamma_7}{2.7/\xi}\Delta T, \tag{2}$$

with the collision rate per Li atom $\Gamma_7=\frac{\Gamma_{coll}}{N_7}$.

Application of this model to the measured data results in values for $|a_{7,87}|$ and are summarized in Table I.

A correction has to be applied to the ballistic expansion time for the Li component. This is because the self-inductance of the trap coils results in a coil current shutdown time scale on the order of 200 $\mu$s. The cloud of Li atoms already starts to expand during this turn-off process whereby the effective time of flight is larger than the nominal value. Hence, the temperatures derived from the Gaussian widths of the Li clouds using the nominal time-of-flight value are overestimated. Therefore, an additional experimentally determined correction to the time of flight of 130 $\mu$s is added to the nominal time of flight of 1000 $\mu$s. This changes the measured temperatures by up to 25% for low temperatures as compared to uncorrected values. For very slow evaporation ramps, where Li and Rb are in constant equilibrium, this correction yields the same values for both temperatures. The delayed turn-off effect is negligible for the heavier Rb atoms which we let expand for a much longer time (20 ms).

The error introduced due to inexact values for the temperature difference can be estimated by applying a small temperature offset to the measured temperature evolution. The effect on the derived scattering length for $T_1=10$ $\mu$K is shown in Fig. 2(a). Mismatched temperature estimates of only 200 nK in either direction result in variations in $|a_{7,87}|$ of up to $9a_B$ for individual $T_1$ measurements. This strongly limits the accuracy to which we can reliably determine $|a_{7,87}|$. We conservatively estimate $\epsilon_{dT}\approx 18a_B$ by taking the residual shot-to-shot fluctuations after the correction for time of flight of the Li of $\Delta T\approx 500$ nK as a measure for the remaining temperature mismatch.

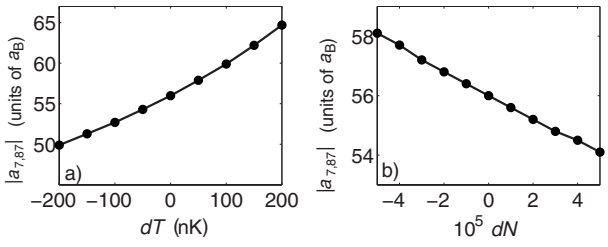


FIG. 2. Uncertainty in the temperature difference (a) and Rb atom numbers (b) introduce uncertainty in the derived scattering length. Data for $T_1=10$ $\mu$K are shown. The values are determined by varying the measured $\Delta T$ and $N_{87}$ by small amounts $dT$ and $dN$ and performing the fit to the altered data as in Fig. 1. The influence of the uncertainty $dN$ is small compared to that of the uncertainty $dT$.

Another uncertainty, $\epsilon_{dN}\approx 1a_B$, derives from the Rb atom numbers, but this contribution $(\delta|a_{7,87}|/dN\approx 0.5a_B/10^5)$ is small compared to the error introduced due to the residual Li temperature fluctuations [Fig. 2(b)]. The total error in $|a_{7,87}|$ is then $\epsilon_{7,87}=\sqrt{\epsilon_{\bar{a}}^2+\epsilon_{dT}^2+\epsilon_{dN}^2}\approx 19a_B$, where $\epsilon_{\bar{a}}=5.2a_B$ is the standard deviation of the best fit values averaged over the three thermalization measurements. Hence, the result of the thermalization experiments is $|a_{7,87}|=(59\pm 19)a_B$.

Uncertainties in the determination of the total Li atom number that will be discussed in Sec. IV in detail have negligible effect on the error bar of $|a_{7,87}|$. This is due to the much larger Rb density making the probability of a Li and a Rb atom meeting in the same position in the trap much higher than that of two Li atoms. Furthermore, the Li-Li scattering cross section is much smaller, reducing the Li-Li collision rate further. Numerical checks were performed to verify that these collisions can be safely ignored.

This result for $|a_{7,87}|$ does not agree well with calculations based on *ab initio* scattering potentials [24], which predict $a_{7,87}=-0.25a_B$. With such a value we would not have seen any interspecies thermalization on the time scale of our experimental cycle. The deviation is likely to be due to the very imprecise theoretical knowledge of the scattering potentials. Probably the good agreement for the measured $^6$Li-$^{87}$Rb scattering length [4] with the theoretical value presented in [24] is coincidental.

## IV. EVIDENCE FOR COLLAPSE OF THE Li COMPONENT

Upon cooling the Rb to even lower temperatures than for the above thermalization measurements, we reach a regime where we approach $T_c$ for Bose-Einstein condensation of Li. Unlike $^{87}$Rb, due to their attractive scattering length of $a_7=-27.3a_B$, pure condensates of $^7$Li are unstable against collapse. However, the kinetic pressure in a trapped condensate allows for a certain maximum number of condensed atoms [14,15,25]. An estimate of the maximum atom number in a stable Li condensate for our trapping geometry gives a value of $N_{max}\approx\frac{a_{ho,7}}{|a_7|}\approx 700$. Here, $a_{ho,7}$ is the length scale of the Li harmonic oscillator ground state. The resolution in detecting atom numbers with our absorption imaging is insufficient to resolve such small atomic samples. However, observation of a sudden drop in the Li atom number for temperatures lower than 1.5 $\mu$K (Fig. 3) provides a means of revealing criticality. Upon reaching the critical temperature for the Bose-Einstein transition, Li atoms begin to accumulate in the ground state of the trap, forming a small condensate. The more atoms condense, the stronger the condensate is contracted to a size smaller than the harmonic oscillator ground state [14]. Eventually, the condensate becomes mechanically unstable and collapses upon itself, thereby strongly increas-

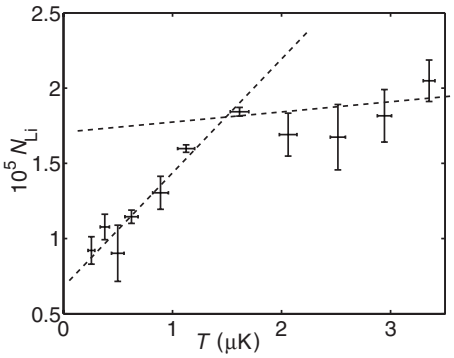


FIG. 3. The Li atom number drops drastically for temperatures lower than 1.5 $\mu$K. The resulting critical atom number $N_{c,7} \approx 6 \times 10^5$ is larger by a factor of 4 than the measured value. Possible calibration uncertainties are discussed in the text. The dashed lines are to guide the eye.

ing the density and thus the rate of three-body recombinations. Depending on the conditions, collective decay may also be important or even predominant [26,27]. All condensed atoms are removed from the trap because the energy released in these inelastic processes is much larger than the trap depth. A new condensate is formed on the time scale of thermalization. With each collapse, this process is repeated, as long as the thermal cloud of Li atoms is overcritical with respect to Bose-Einstein condensation. This therefore poses a permanent loss channel for the much larger number of thermal Li atoms. Depending on the thermalization rate, the overall decay time can be on the order of a hundred milliseconds [18] or many tens of seconds [15]. In our case, we have high trap frequencies and large thermalization rates. We therefore expect this process to be rapid.

While the time-of-flight correction for the Li atoms works well for the temperature range used in the thermalization experiments, in the low temperature regime we still see a discrepancy between $T_{87}$ and $T_7$. We observe $T_{87} < T_7$ even though we explicitly took care to ensure thermal equilibrium. We hence assume $T_7 = T_{87}$ for this experiment and plot the Li data against $T_{87}$ (Fig. 3). With the approximate value of the measured $T_{c,7} \approx 1.5$ $\mu$K we derive a critical atom number of $N_{c,7} = 1.2\left(\frac{k_B T_{c,7}}{\hbar \bar{\omega}_7}\right)^3 \approx 6 \times 10^5$, which is a factor of 4 larger than the measured atom number.

If we assume that the losses are really due to a collapse at $T = 1.5$ $\mu$K, the small number of measured atoms needs an explanation. This number can be experimentally underestimated if the Li atoms do not remain in the cycling transition used for imaging for the whole duration of the optical pulse. The cloud then becomes transparent for the imaging beam yielding less optical density and lower atom numbers. We have checked the dependence on the Li imaging repumper power and found a roughly exponential saturation behavior. Normal imaging is performed with a repumper power in the saturated regime giving confidence in complete repumping during the imaging process. Nonetheless, the imaging process is also subject to a time-dependent Doppler shift due to photon recoil during photon scattering affecting light Li atoms particularly strongly. In order to reduce this effect to first order, repumping and probe beams are aligned antiparallel.

The Li absorption imaging incongruity as such is not new but manifests itself strongly under our experimental conditions. Experimental optimization trying to balance the different pumping and heating effects during the imaging pulse for both $^6$Li and $^7$Li has been discussed in [28]. Here, an atom number uncertainty by a factor of 2 is quoted. In the group in Innsbruck, similar observations have been made with $^6$Li [29]. Other groups also working with $^6$Li image at high magnetic offset fields close to the interesting Feshbach resonance at 822 G [30], where the Paschen-Back effect detunes the overlapping resonances. Full cycling transitions are possible in this case, thus avoiding the need for a repumper. The Li atoms are nonetheless subject to recoil Doppler shifts. A full description including the named effects is necessary to quantitatively study their influences on the effective time-dependent absorption cross section. To this end, a separate publication is under preparation [31,32].

As an alternative to Bose-Einstein criticality, increased losses could also arise because of strongly energy-dependent three-body loss coefficients that derive from a Feshbach resonance at low magnetic fields similar to the case of Cs [33]. This hypothesis can be safely discarded as a mixture of stretched states can in principle not experience such interaction resonances. Yet there may still be a very small fraction of atoms in the undesired spin states such as $|2,1\rangle$ below our detection limit causing residual losses. Even though this cannot be ruled out, it is more likely that as yet unaccounted for effects during the imaging pulse cause incorrect atom number determinations and that Bose-Einstein criticality is indeed reached [34].

We have experimentally checked for inelastic losses in the mixture in the temperature range between 15 $\mu$K and 3 $\mu$K. We find that the lifetime of Li in the mixture is reduced for colder temperatures, but still remains on a time scale of seconds. Going back to the data presented in Fig. 3, there, cooling of the mixture from 4 $\mu$K to any lower value is done in only 500 ms leading to the observed drastic losses. We therefore conclude that inelastic collisions at thermal densities cannot account for the sudden change in behavior of the data below 1.5 $\mu$K unless another loss channel (condensate collapse) opens. We attribute this loss channel to be due to the creation and subsequent annihilation of Li condensates rapidly depleting the observable number of residual thermal atoms on a short time scale.

## V. MEAN-FIELD STABILIZATION

However, the situation may change dramatically in the presence of a second *degenerate* species. The mean-field energy can be either increased or decreased depending on the interaction with the second species. If the second species itself forms a stable condensate, as is the case for $^{87}$Rb, it depends on the sign of the interspecies scattering length, whether the collapse of the first species is accelerated or slowed down [35]. For our system this means that for $a_{7,87} < 0$ even very small Li condensates are unstable, as for $a_{7,87} > 0$ larger metastable Li condensates can be supported.

To demonstrate this we solve the following coupled Gross-Pitaevskii equation for the spherically symmetric case:

$$\left(-\frac{\hbar}{2m_k}\frac{1}{r}\frac{d^2}{dr^2}r+\frac{m_k}{2}\tilde{\omega}_k^2r^2+g_kN_k+g_{7,87}N_{l\neq k}\right)\psi_k=\mu\psi_k, \tag{3}$$

for $k,l=7$ or 87. Here $g_k=4\pi\hbar^2a_k/m_k$, $g_{7,87}=2\pi\hbar^2a_{7,87}\frac{m_7+m_{87}}{m_7m_{87}}$, and $N_{k,l}$ are the atom numbers of both species.

To find the ground state of the system, we use the method of steepest gradient [36]. It has already been successfully employed to study mixed systems of degenerate bosons and fermions [37,38]. Based on evaluating the energy functionals $H_k[\psi_k,\psi_l]$, their minimal values are found by propagating the wave functions along the direction of the gradient $\frac{\delta H_k}{\delta\psi_k}$ using small time steps $d\tau$,

$$\psi_k'\rightarrow\psi_k+d\tau\frac{\delta H_k}{\delta\psi_k}. \tag{4}$$

Formally, this corresponds to replacing the real time dependence in the Gross-Pitaevskii equation by an imaginary time dependence $\tau=it$. Under the constraint that the normalization of $\psi_k'$ does not change, which one ensures by explicitly normalizing $\psi_k'$ after each propagation step, this method is self-consistent. The final result does not depend on the initial trial functions, but a sensible choice may significantly reduce the integration time needed for convergence. We use the ground-state wave functions of the respective harmonic trap potentials as $\psi_k(\tau=0)$, which are normalized Gaussian functions.

For simplicity we restrict the calculation to the spherically symmetric case $V_k(\vec{r})=\frac{1}{2}m_k\tilde{\omega}_k^2r^2$, where we use the mean trap frequencies $\tilde{\omega}_k=(\omega_{k,r}^2\omega_{k,z})^{1/3}$.

The space coordinate was discretized with step size $dr=0.1$ $\mu$m up to $r=40$ $\mu$m, which corresponds to $41.9a_{ho,87}$ and $22.3a_{ho,7}$. Time was discretized using $d\tau=5\times10^{-7}$ s and the propagation was performed for 6000 time steps.

For $a_{7,87}=0$, we obtain the critical atom number for stable Li condensates by increasing $N_7$ to the point where we obtain no numerically stable solution to the above equation. We find a value close to the estimated 700 atoms for our trap conditions. Setting the mutual interaction to repulsive interaction using the measured absolute value to $a_{7,87}=+59a_B$ results in a demixing of the two condensates and a substantial increase in the maximum allowed number of condensed Li atoms (Fig. 4).

The quoted method only finds the ground state of a given system. For situations where collapse occurs, it is not suitable to accurately describe the ongoing complex dynamics. Powerful numerical schemes based on the Crank-Nicholson scheme [35,39,40] have been developed for studying these dynamics, but these go beyond the scope of this publication. Here we restrict ourselves to the static stabilization of Li condensates in the presence of a Rb condensate. Our results may experience modifications when considering the cylindrically symmetric trap employed in our experiment [41]. Also, different gravitational sags for the two species may affect the overall stabilization. This is suggested by experimental results presented by Hall *et al.* [42]. They showed that the mutual interaction between condensates in the two hyperfine

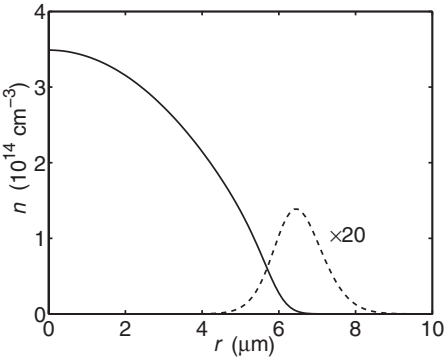


FIG. 4. Condensate densities of $1.5\times10^5$ Rb $|2,2\rangle$ (solid line) and 6000 mean-field stabilized Li $|2,2\rangle$ atoms (dashed line) with trap parameters from our experiment. The interspecies mean-field forces the Li condensate into a shell around a large Rb nucleus. The resulting density reduction allows for a much larger condensate to survive than in the absence of Rb.

states of Rb caused a spherically symmetric phase-separated state in the case of vanishing relative gravitational sag. Introduction of a small gravitational sag of 0.4 $\mu$m, which was smaller than the Thomas-Fermi radii of the condensates involved, caused strongly damped dynamics and led to a vertically phase-separated state with only limited spatial overlap between the two condensates. Calculations incorporating the effect of gravity will have to be performed to clarify whether or not mean-field stabilization then is still significant. In order to ensure symmetry as much as possible, tightly confining traps with strongly reduced relative gravitational sag should be employed to study mean-field stabilization.

Based on the hypothesis that $a_{7,87}$ is positive, we performed a series of experiments where both Li and Rb are slowly cooled to about 3 $\mu$K, which is well above the experimentally determined value of the critical temperature for Li condensation. The respective critical temperatures behave as $T_{c,7}=\sqrt{\frac{87}{7}}\left(\frac{N_7}{N_{87}}\right)^{1/3}T_{c,87}$. The large mass ratio and the therefore strongly different trap frequencies lead to a higher critical temperature for Li given our experimental conditions, i.e., $T_{c,7}\approx1.5$ $\mu$K, while $T_{c,87}\approx0.7$ $\mu$K. In order to generate a Rb condensate without losing too many Li atoms during the evaporation to $T_{c,87}$, we very quickly (within 200 ms) cool the Rb component into degeneracy. The evaporating microwave knife remains activated at the end of the evaporation ramp resulting in a slow temperature decrease from initially 800 nK down to about 200 nK during the 900 ms storage time. During the storage stage Rb condensates with atom numbers ranging from some $10^4$ up to $1.5\times10^5$ atoms are formed. The atom number of the Li component drops sharply to less than $10^4$ at the end of the 900 ms and no bimodal density distribution, the typical sign for Bose-Einstein condensation, was observed at any time for the Li component. Extraction of the Li temperature from the time-of-flight images renders values around 1 $\mu$K throughout the duration of the experiment, while the collisional thermalization model suggests that the thermalization is very fast so that $\Delta T<100$ nK for $t>200$ ms. Specifically, the amount of Rb atoms during the experiment is sufficient to ensure thermalization *even* with an underestimation of the Li atom num-

ber by a factor of 4. We therefore believe that the Li temperatures derived from Li absorption imaging at low temperatures are not reflecting the actual temperature of the species. Accurate values for very low Li temperatures seem to be not achievable under current conditions. A conclusion as to the sign of the scattering length at this stage is not possible. Two possible scenarios remain as follows:

(a) The sign is positive, but the relative gravitational sag reduces the overlap so that stabilization is suppressed. The Li condensates stay below the detection limit.

(b) The sign is negative and the Li condensates are made even more unstable rendering them unresolvable for our system.

To reduce the effects of gravity on the overlap of the atomic clouds, one should perform these experiments again in much tighter confinement. The different trap geometry, cigar shaped as opposed to spherically symmetric, has to be considered in the theoretical description as well, to obtain a better quantitative picture of mean-field stabilization under our experimental conditions.

## VI. CONCLUSION AND OUTLOOK

In conclusion, we cooled a mixed gas of two atomic species, $^7$Li and $^{87}$Rb, down to ultracold temperatures. We determined the absolute value of the pure triplet interspecies scattering $|a_{7,87}|$ through measurements of the thermalization speed to be $59 \pm 19$ Bohr radii. The cause of slow atom losses experienced by the Li during the cooling process remains unclear. As Li and Rb atoms in other states than $|2,2\rangle$ are kept below our detection limit direct inelastic loss processes can be ruled out. Sudden severe Li losses upon cooling below a critical temperature are interpreted as the onset of Bose-Einstein condensation for the Li component. Even though numerical mean-field calculations suggest increased stabilization of the Li condensate in the case of repulsive interspecies interaction, Li condensates in the presence of a Rb condensate were not detected even in the case of large Rb condensates. Such an observation directly determines the sign of the interspecies interaction to be positive whereas from the current observational viewpoint no decisive conclusion as to the sign of $a_{7,87}$ can be made. The effects of the different trap geometry and of gravitational sag need to be taken into account for more accurate quantitative predictions. More tightly confining traps that reduce the effect of gravity may then prove to be more suitable to study mean-field stabilization. A detailed study of the imaging process of Li at low magnetic fields is under preparation addressing the atom number inconsistencies [32].

## ACKNOWLEDGMENT

This work has been supported by the Deutsche Forschungsgemeinschaft (DFG).

[1] A. G. Truscott, K. E. Strecker, W. I. McAlexander, G. B. Partridge, and R. G. Hulet, Science **291**, 2570 (2001).
[2] Z. Hadzibabic, C. A. Stan, K. Dieckmann, S. Gupta, M. W. Zwierlein, A. Görlitz, and W. Ketterle, Phys. Rev. Lett. **88**, 160401 (2002).
[3] G. Roati, F. Riboli, G. Modugno, and M. Inguscio, Phys. Rev. Lett. **89**, 150403 (2002).
[4] C. Silber, S. Günther, C. Marzok, B. Deh, Ph. W. Courteille, and C. Zimmermann, Phys. Rev. Lett. **95**, 170408 (2005).
[5] J. M. McNamara, T. Jeltes, A. S. Tychkov, W. Hogervorst, and W. Vassen, Phys. Rev. Lett. **97**, 080404 (2006).
[6] C. J. Myatt, E. A. Burt, R. W. Ghrist, E. A. Cornell, and C. E. Wieman, Phys. Rev. Lett. **78**, 586 (1997).
[7] I. Bloch, M. Greiner, O. Mandel, T. W. Hänsch, and T. Esslinger, Phys. Rev. A **64**, 021402(R) (2001).
[8] G. Modugno, G. Ferrari, G. Roati, R. J. Brecha, A. Simoni, and M. Inguscio, Science **294**, 1320 (2001).
[9] G. Ferrari, M. Inguscio, W. Jastrzebski, G. Modugno, G. Roati, and A. Simoni, Phys. Rev. Lett. **89**, 053202 (2002); G. Modugno, M. Modugno, F. Riboli, G. Roati, and M. Inguscio, *ibid.* **89**, 190404 (2002).
[10] G. Roati, M. Zaccanti, C. D'Errico, J. Catani, M. Modugno, A. Simoni, M. Inguscio, and G. Modugno, arXiv:cond-mat/0703714v1.
[11] M. Anderlini, E. Courtade, M. Cristiani, D. Cossart, D. Ciampini, C. Sias, O. Morsch, and E. Arimondo, Phys. Rev. A **71**, 061401(R) (2005).
[12] Y. Takasu, T. Fukuhara, M. Kitagawa, M. Kumakura, and Y. Takahashi, Laser Phys. **16**, 713 (2006).
[13] S. Tassy, N. Nemitz, F. Baumer, C. Höhl, A. Batär, and A. Görlitz, e-print arXiv:0709.827v1.
[14] P. A. Ruprecht, M. J. Holland, K. Burnett, and M. Edwards, Phys. Rev. A **51**, 4704 (1995).
[15] C. A. Sackett, C. C. Bradley, M. Welling, and R. G. Hulet, Appl. Phys. B: Lasers Opt. **65**, 433 (1997).
[16] J. L. Roberts, N. R. Claussen, S. L. Cornish, E. A. Donley, E. A. Cornell, and C. E. Wieman, Phys. Rev. Lett. **86**, 4211 (2001).
[17] E. A. Donley, N. R. Claussen, S. L. Cornish, J. L. Roberts, E. A. Cornell, and C. E. Wieman, Nature (London) **412**, 295 (2001).
[18] S. K. Adhikari, Phys. Lett. A **281**, 265 (2001).
[19] As the two magneto-optical traps strongly interact inelastically in the short compressed stage, the Li atom number can be a factor of 4 higher when we do not load Rb.
[20] S. Günther, Ph.D. thesis, Universität Tübingen, 2006.
[21] G. Delannoy, S. G. Murdoch, V. Boyer, V. Josse, P. Bouyer, and A. Aspect, Phys. Rev. A **63**, 051602(R) (2001).
[22] A. Mosk, S. Kraft, M. Mudrich, K. Singer, W. Wohlleben, R. Grimm, and M. Weidemüller, Appl. Phys. B: Lasers Opt. **73**, 791 (2001).
[23] Huang Wu and Ch. J. Foot, J. Phys. B **29**, L321 (1996).
[24] H. Ouerdane and M. J. Jamieson, Phys. Rev. A **70**, 022712 (2004).
[25] T. Bergeman, Phys. Rev. A **55**, 3658 (1997).
[26] H. T. C. Stoof, J. Stat. Phys. **87**, 1353 (1997).

[27] C. A. Sackett, H. T. C. Stoof, and R. G. Hulet, Phys. Rev. Lett. **80**, 2031 (1998).
[28] F. Schreck, Ph.D. thesis, Université Paris VI, 2002.
[29] R. Grimm (private communication).
[30] M. W. Zwierlein, C. A. Stan, C. H. Schunck, S. M. F. Raupach, A. J. Kerman, and W. Ketterle, Phys. Rev. Lett. **92**, 120403 (2004).
[31] Incorporation of time-dependent Doppler shifts into the imaging process on the $D2$ line is in principle possible, but the unresolved hyperfine structure of Li makes the full description quite involved. In the case of $^{6}$Li, 18 states have to be taken into account resulting in a Bloch matrix of rank 324. For $^{7}$Li, even 24 states need to be considered, increasing the rank to 576. A separate publication dedicated to this problem is under preparation as its complexity exceeds the scope of this submission.
[32] B. Deh, C. Marzok, C. Zimmermann, and Ph. W. Courteille (unpublished).
[33] T. Weber, J. Herbig, M. Mark, H.-C. Nägerl, and R. Grimm, Phys. Rev. Lett. **91**, 123201 (2003).
[34] We experienced similar Li atom number inconsistencies in our study of the fermionic species $^{6}$Li when considering Fermi degeneracy. $^{6}$Li also has an unresolved hyperfine structure of the excited $2\,^{3}P_{1}$state.
[35] S. K. Adhikari, Phys. Rev. A **63**, 043611 (2001).
[36] F. Dalfovo and S. Stringari, Phys. Rev. A **53**, 2477 (1996).
[37] R. Roth, Phys. Rev. A **66**, 013614 (2002).
[38] M. Modugno, F. Ferlaino, F. Riboli, G. Roati, G. Modugno, and M. Inguscio, Phys. Rev. A **68**, 043626 (2003).
[39] F. Dalfovo and M. Modugno, Phys. Rev. A **61**, 023605 (2000).
[40] M. Holland and J. Cooper, Phys. Rev. A **53**, R1954 (1996).
[41] B. D. Esry, C. H. Greene, J. P. Burke, Jr., and J. L. Bohn, Phys. Rev. Lett. **78**, 3594 (1997).
[42] D. S. Hall, M. R. Matthews, J. R. Ensher, C. E. Wieman, and E. A. Cornell, Phys. Rev. Lett. **81**, 1539 (1998).